

# Quassinoids from *Picrasma quassioides* and Their Neuroprotective Effects

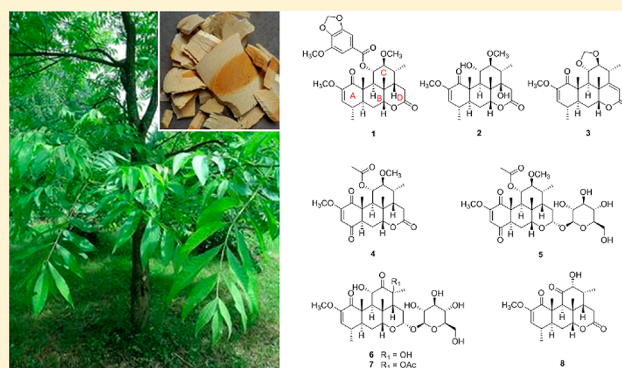
Wen-Yu Zhao,<sup>†,‡</sup> Xiao-Yu Song,<sup>†,‡</sup> Lu Zhao,<sup>†,‡</sup> Chun-Xin Zou,<sup>†,‡</sup> Wei-Yu Zhou,<sup>†,‡</sup> Bin Lin,<sup>‡,§</sup> Guo-Dong Yao,<sup>†,‡</sup> Xiao-Xiao Huang,<sup>\*,†,‡,⊥</sup> and Shao-Jiang Song<sup>\*,†,‡</sup> 

<sup>†</sup>School of Traditional Chinese Materia Medica, <sup>‡</sup>Key Laboratory of Computational Chemistry-Based Natural Antitumor Drug Research & Development, Liaoning Province, and <sup>§</sup>School of Pharmaceutical Engineering, Shenyang Pharmaceutical University, Shenyang 110016, People's Republic of China

<sup>⊥</sup>Chinese People's Liberation Army 210 Hospital, Dalian 116021, People's Republic of China

## Supporting Information

**ABSTRACT:** Quassinoids are a class of highly oxygenated degraded triterpenoids exclusively discovered from plants of the Simaroubaceae family. In this study, eight new (1–8) and 15 known quassinoids (9–23) were isolated from an extract of the stems of *Picrasma quassioides*. The structures were elucidated by spectroscopic analysis and electronic circular dichroism spectra combined with quantum chemical calculations. Compounds 4 and 5 represent the first examples of 18-nor-quassinoids from *P. quassioides*. All isolates were screened for their neuroprotective activities toward H<sub>2</sub>O<sub>2</sub>-induced cell damage in SH-SY5Y cells. Further study revealed that the potential protective activities of these compounds appeared to occur via the suppression of cell apoptosis and downregulation of caspase-3 activation.



*Picrasma quassioides* (D. Don) Benn. (family Simaroubaceae) is widely distributed in Korea, Japan, and southern China.<sup>1</sup> The stems of *P. quassioides*, commonly known as Kumu in Chinese, have historically been used as a source of anti-inflammatory, insecticidal, and antibacterial compounds.<sup>2</sup> Previous chemical research of *P. quassioides* led to the isolation of quassinoids,<sup>1</sup> triterpenoids,<sup>2</sup> alkaloids,<sup>3</sup> and phenolic glycosides.<sup>4</sup> Quassinoids are triterpenoids biogenetically derived from (20R)-euphol or (20S)-tirucalol in the Simaroubaceae family of plants.<sup>5</sup> Five groups of representative skeletons have been reported, C<sub>18</sub>, C<sub>19</sub>, C<sub>20</sub>, C<sub>22</sub>, and C<sub>25</sub> types, according to the number of carbons in the main chain.<sup>6,7</sup> In view of their structural diversity and potential medicinal value, we focused on quassinoids from *P. quassioides* as part of a continuing search for structurally unique and bioactive metabolites from nature.

In this study, eight new quassinoids, along with 15 known analogues, including C<sub>19</sub>, C<sub>20</sub>, and C<sub>25</sub> derivatives, were isolated and identified from the stems of *P. quassioides*. Among them, quassin (13) is the first quassinoid discovered in the C<sub>20</sub> group, and its absolute configuration was established by applying the electronic circular dichroism (ECD) exciton chirality method (ECM).<sup>8</sup> Since then, the absolute configurations of other structurally similar analogues have been defined by different methods, mainly biosynthetic considerations and comparisons of the ECD spectra with literature data.<sup>9–12</sup> However, recent reports by Pescitelli and Di Bari showed that the method of using ECM or empirical correlations of ECD without considering structural

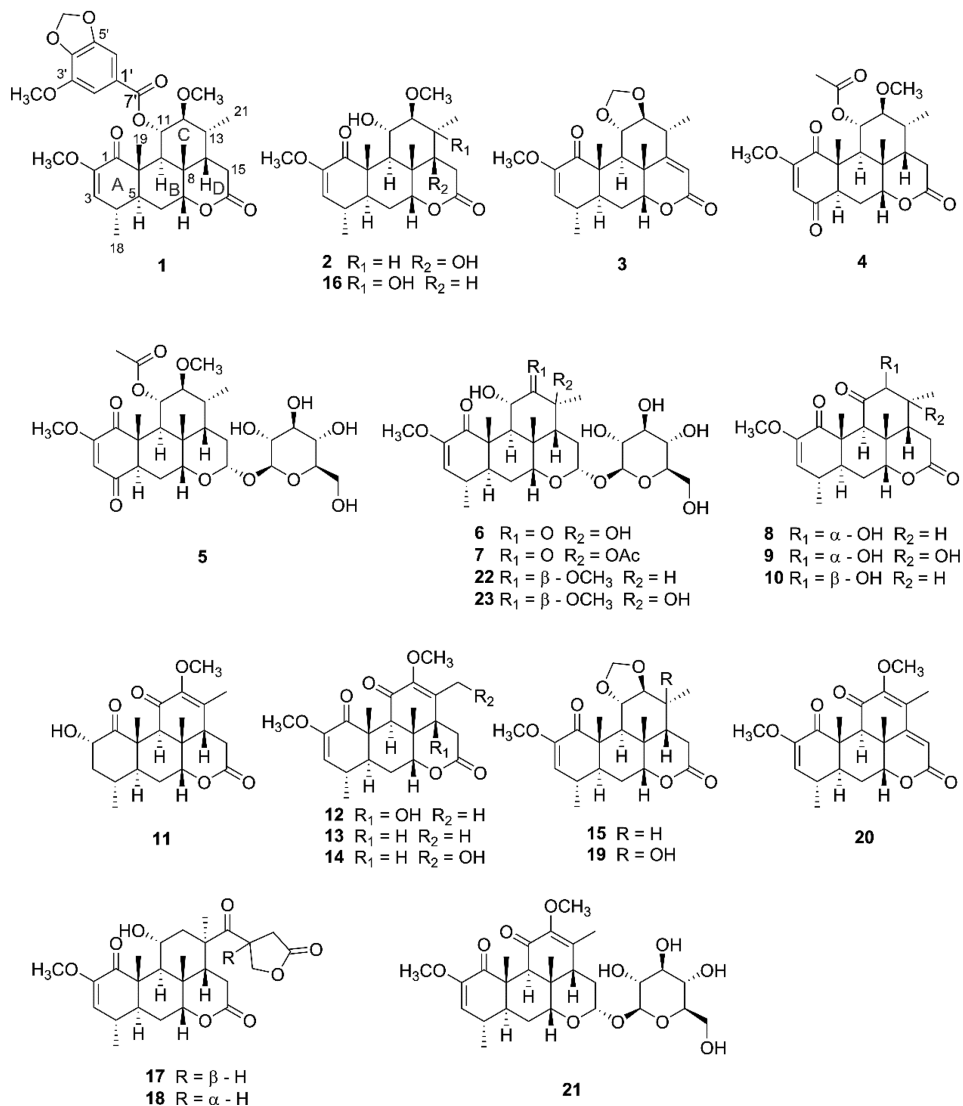
changes is unreliable.<sup>13,14</sup> Inspired by this, quantum chemical calculations were performed to determine the absolute configuration of each new quassinoid in this study. The protective effects of all isolates were screened against human neuroblastoma SH-SY5Y cell injury induced by H<sub>2</sub>O<sub>2</sub>.

## RESULTS AND DISCUSSION

Kumulactone A (1) had the molecular formula C<sub>31</sub>H<sub>38</sub>O<sub>10</sub>, deduced from its sodium adduct ion [M + Na]<sup>+</sup> at *m/z* 593.2338 (calcd for C<sub>31</sub>H<sub>38</sub>O<sub>10</sub>Na 593.2357) in its HRESIMS data, which indicated 13 indices of hydrogen deficiency. Its IR spectrum showed peaks characteristic of the presence of carbonyl groups (1732 and 1705 cm<sup>-1</sup>) and an aromatic ring (1610 cm<sup>-1</sup>). The <sup>1</sup>H NMR data (Table 1) displayed two aromatic protons at δ<sub>H</sub> 7.30 (d, *J* = 1.4 Hz) and 7.09 (d, *J* = 1.4 Hz) and signals typical of a methylenedioxy moiety at δ<sub>H</sub> 6.10; three methoxy groups at δ<sub>H</sub> 3.93, 3.35, and 3.14; two tertiary methyls at δ<sub>H</sub> 1.22 and 1.17; and two secondary methyls at δ<sub>H</sub> 1.02 (d, *J* = 6.8 Hz) and 0.92 (d, *J* = 6.6 Hz). The <sup>13</sup>C NMR (Table 2) and HSQC data of 1 exhibited 31 carbon resonances including three carbonyl carbons (δ<sub>C</sub> 200.0, 169.9, and 164.5), six aromatic carbons (δ<sub>C</sub> 148.3, 142.9, 139.1, 124.0, 110.0, and 103.1), an olefinic group (δ<sub>C</sub> 147.8 and 114.7), a methylenedioxy carbon (δ<sub>C</sub> 102.3), six oxygenated carbons (δ<sub>C</sub> 84.3, 81.0, 73.2,

Received: June 7, 2018

Chart 1

Table 1. <sup>1</sup>H NMR (400 MHz) Data of Compounds 1–8 (δ in ppm, J in Hz)

position	1 <sup>a</sup>	2 <sup>b</sup>	3 <sup>b</sup>	4 <sup>b</sup>	5 <sup>a</sup>	6 <sup>a</sup>	7 <sup>a</sup>	8 <sup>a</sup>
3	5.30, d (2.5)	5.44, d (2.5)	5.23, d (2.5)	5.87, s	5.88, s	5.53, d (2.5)	5.53, d (2.5)	5.58, d (2.4)
4	2.40, m	2.53, m	2.42, m			2.45, m	2.44, m	2.38, m
5	1.91, m	1.90, m	1.90, m	2.40, m	2.27, dd (6.1, 2.1)	1.73, m	1.69, m	1.56, m
6a	1.92, m	2.10, dt (14.4, 3.7)	2.94, m	3.07, ddd (15.4, 2.8, 2.1)	2.50, m	1.93, m	1.98, m	1.92, m
6b	1.83, m	1.75, ddd (14.4, 12.9, 2.0)	2.22, m	2.17, m	2.11, m	1.72, m	1.70, m	1.91, m
7	4.31, br s	4.59, dd (3.7, 2.0)	4.24, br s	4.28, t (2.8)	3.33, overlap	3.35, br s	3.38, br s	4.37, br s
9		2.05, m	2.28, d (11.4)	2.59, d (11.6)	3.01, d (12.0)	2.34, d (12.0)	2.32, d (12.0)	2.78, s
11	5.33, m	3.76, m	3.82, dd (11.4, 8.3)	5.25, dd (11.6, 8.7)	4.99, dd (12.0, 8.8)	4.91, t (12.0)	4.62, t (12.0)	
12	3.41, m	2.71, m	3.01, m	2.96, dd (11.4, 8.7)	2.89, dd (11.4, 8.8)			3.99, d (5.3)
13	2.13, m	1.90, m	2.94, m	2.17, m	2.01, m			2.07, m
14	1.55, ddd (12.8, 9.9, 3.9)			1.81, ddd (12.2, 7.8, 4.5)	1.46, m	1.86, dd (13.6, 4.6)	2.27, dd (13.5, 4.6)	1.78, ddd (14.8, 7.1, 3.4)
15a	2.63, dd (19.4, 9.9)	2.71, d (18.9)	5.86, d (1.2)	2.63, m	1.55, m	1.51, m	1.53, m	2.92, dd (15.7, 7.1)
15b	2.51, overlap	2.55, d (18.9)		2.40, m	1.37, m	0.92, m	0.93, m	2.38, dd (15.7, 3.4)
16					4.77, m	4.79, dd (9.8, 2.4)	4.83, dd (9.7, 2.4)	
18	1.02, d (6.8)	1.13, d (6.4)	1.14, d (6.9)			1.02, d (6.8)	1.02, d (6.9)	1.07, d (6.8)
19	1.17, s	1.48, s	1.39, s	1.38, s	1.15, s	1.39, s	1.36, s	1.50, s

Table 1. continued

position	1 <sup>a</sup>	2 <sup>b</sup>	3 <sup>b</sup>	4 <sup>b</sup>	5 <sup>a</sup>	6 <sup>a</sup>	7 <sup>a</sup>	8 <sup>a</sup>
20	1.22, s	1.14, s	1.33, s	1.32, s	1.09, s	1.48, s	1.38, s	1.03, s
21	0.92, d (6.6)	1.06, d (6.6)	1.30, d (6.0)	0.99, d (6.7)	0.87, d (6.6)	1.11, s	1.26, s	0.92, d (6.6)
2-OMe	3.35, s	3.58, s	3.56, s	3.83, s	3.79, s	3.48, s	3.48, s	3.47, s
12-OMe	3.14, s	3.63, s		3.36, s	3.20, s			
–OCH <sub>2</sub> O–	6.10, s		5.22, br s, 5.06, br s					
–OAc				2.00, s	1.87, s		2.09, s	
1'					4.44, d (7.9)	4.38, d (7.8)	4.38, d (7.8)	
2'	7.09, d (1.4)				2.96, m	2.91, m	2.90, m	
3'					3.07, m	3.06, m	3.06, m	
4'					3.04, m	3.00, m	3.00, m	
5'					3.19, m	3.11, m	3.11, m	
6'	7.30, d (1.4)				3.65, m	3.64, m	3.64, m	
					3.42, m	3.41, m	3.41, m	
3'-OCH <sub>3</sub>	3.93, s							

<sup>a</sup>Measured in DMSO-*d*<sub>6</sub>. <sup>b</sup>Measured in CDCl<sub>3</sub>.

Table 2. <sup>13</sup>C NMR (100 MHz) Data of Compounds 1–8 ( $\delta$  in ppm)

position	1 <sup>a</sup>	2 <sup>b</sup>	3 <sup>bc</sup>	4 <sup>b</sup>	5 <sup>a</sup>	6 <sup>a</sup>	7 <sup>a</sup>	8 <sup>a</sup>
1	200.0	205.3	197.9	199.0	200.3	204.0	204.1	197.1
2	147.8	148.1	148.5	164.1	162.9	147.6	147.5	146.9
3	114.7	118.9	114.9	109.3	109.6	118.0	117.9	118.7
4	31.1	31.9	32.4	193.3	193.6	31.4	31.4	30.3
5	42.8	43.3	43.2	50.2	49.7	43.8	43.8	43.3
6	24.8	25.0	25.6	24.2	23.6	24.8	24.9	24.8
7	81.0	78.7	78.4	82.1	76.0	76.3	75.5	78.5
8	35.3	40.4	39.7	35.7	36.6	37.1	37.0	39.5
9	34.7	38.8	41.1	38.6	38.0	41.8	42.6	46.6
10	46.2	47.8	46.3	49.3	48.8	48.2	48.3	46.6
11	73.2	73.5	77.0	71.4	71.8	70.2	70.5	211.1
12	84.3	89.0	86.0	84.9	84.6	211.0	206.5	73.9
13	34.4	43.1	37.5	33.3	32.6	78.7	86.7	37.5
14	44.1	74.7	164.5	45.6	46.8	53.8	52.2	43.4
15	27.7	36.4	113.6	27.5	27.0	29.9	28.4	30.3
16	169.9	169.9	167.7	168.8	96.5	97.6	97.2	172.2
18	19.3	19.5	19.8			19.4	19.3	18.9
19	12.1	12.8	12.8	17.1	16.2	12.1	12.0	12.1
20	20.4	15.5	20.9	22.3	20.8	22.9	22.8	24.2
21	13.6	10.6	13.5	14.5	14.7	22.1	17.7	14.7
2-OCH <sub>3</sub>	54.7	55.4	55.1	57.0	56.6	54.8	54.8	54.6
12-OCH <sub>3</sub>	59.5	61.9		59.7	58.2			
–OAc				20.9	20.2		21.3	
				170.3	169.4		169.8	
1'	124.0				97.6	99.0	99.0	
2'	103.1				73.3	73.3	73.2	
3'	142.9				77.0	77.0	77.0	
4'	139.1				70.5	70.0	70.0	
5'	148.3				76.4	76.5	76.4	
6'	110.0				61.1	61.1	61.1	
7'	164.5							
3'-OCH <sub>3</sub>	56.0							
–OCH <sub>2</sub> O–	102.3		96.6					

<sup>a</sup>Measured in DMSO-*d*<sub>6</sub>. <sup>b</sup>Measured in CDCl<sub>3</sub>. <sup>c</sup>Measured at 150 MHz.

59.5, 56.0, and 54.7), two methylene carbons ( $\delta_C$  27.7 and 24.8), five methine carbons ( $\delta_C$  44.1, 42.8, 34.7, 34.4, and 31.1), two quaternary carbons ( $\delta_C$  46.2 and 35.3), and four methyl carbons ( $\delta_C$  20.4, 19.3, 13.6, and 12.1). These characteristic signals implied that **1** was a C<sub>20</sub>-type quassinoid possessing a 3,4-methylenedioxybenzoyl substituent. A comparison of the NMR data of **1** with

those of nigakilactone B<sup>15</sup> revealed that the two compounds had a similar tetracyclic skeleton that differed by a 3-methoxy-4,5-methylenedioxybenzoyl group at C-11, which was confirmed by the HMBC correlation of H-11 with C-7' (Figure 1).

The relative configuration of **1** was determined from a NOESY experiment (Figure 2). The NOESY correlations of

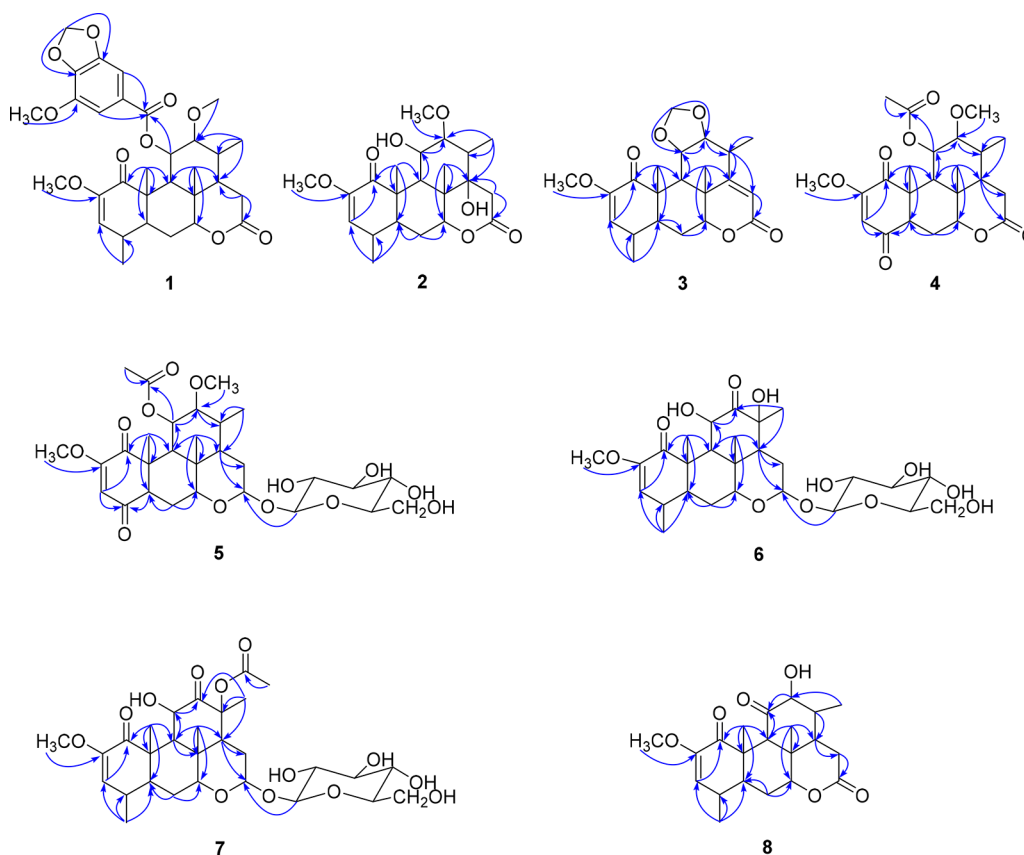


**Figure 1.** Key HMBC correlations for compounds 1–8.

Me-19/H-11, Me-20/H-7, Me-20/H-11, and H-7/H-14 indicated the  $\beta$ -orientation of H-7, H-11, and H-14, while the correlations between Me-21/H-12, H-12/H-9, and Me-18/H-5 established the  $\alpha$ -orientation of H-5, H-9, and H-12.

Kumulactone B (**2**) was assigned the molecular formula  $C_{22}H_{32}O_7$  on the basis of an HRESIMS  $[M + Na]^+$  ion at  $m/z$  431.2054 (calcd 431.2040). An analysis of its NMR data suggested that **2** has the same  $C_{20}$ -type quassinoid skeleton as **1** (Tables 1 and 2). The NMR spectra of **2** were consistent with most of the structural features found in nigakilactone F (**16**),<sup>10</sup> with the major difference being the  $^1H$  NMR chemical shift of Me-21 ( $\delta_H$  1.06, d,  $J = 6.6$  Hz), indicating the absence of a hydroxy group at C-13. Furthermore, the H-13 signal at  $\delta_H$  1.90 and H-15 signals at  $\delta_H$  2.71 and 2.55 were correlated with the signal at  $\delta_C$  74.7 in the HMBC spectrum (Figure 1), suggesting the presence of a hydroxy moiety at C-14.

The NOESY correlations (Figure 2) from Me-20 to H-11 corroborated the  $\alpha$ -orientation of the 11-hydroxy group. The  $\beta$ -orientation of the 12-methoxy group was confirmed by the correlations from H-12 to H-9 and Me-21. The orientation of the HO-14 was difficult to establish directly from the NOESY spectrum due to its connection to a tertiary carbon atom. However, a correlation of Me-21/H-15 was observed, which indicated that C-15 was  $\alpha$ -oriented. In addition, C-15 and HO-14 were on opposite faces of ring D; thus, the orientation of HO-14 was established as being  $\beta$ .

Kumulactone C (**3**) had the molecular formula  $C_{22}H_{28}O_6$  on the basis of its HRESIMS  $[M + Na]^+$  ion at  $m/z$  411.1789 (calcd 411.1778). Its  $^1H$  NMR data (Table 1) showed two olefinic hydrogens at  $\delta_H$  5.86 and 5.23 and the presence of a methylenedioxy group at  $\delta_H$  5.22 and 5.06. The  $^{13}C$  NMR data

(Table 2) in combination with HSQC experiments showed 22 carbon resonances attributable to methoxy ( $\delta_C$  55.1) and methylenedioxy ( $\delta_C$  96.6) moieties and a  $C_{20}$ -type quassinoid skeleton. An analysis of the HMBC spectrum (Figure 1) showed that **3** possessed two  $\alpha,\beta$ -unsaturated carbonyl moieties at C-1, C-2, C-3 and C-14, C-15, C-16. The position of the methylenedioxy group was confirmed by the correlation of the signals at  $\delta_H$  5.22 and 5.06 with C-11 ( $\delta_C$  77.0) and C-12 ( $\delta_C$  86.0). Based on the above evidence, the connectivity of **3** was established. The relative configuration of **3** was confirmed to be the same as those of **1** and **2** based on the results of NOESY experiments (Figure 2).

Kumulactone D (**4**) was determined to have the molecular formula  $C_{23}H_{30}O_8$  from its HRESIMS data ( $[M + Na]^+$   $m/z$  457.1808, calcd 457.1833), which indicated nine indices of hydrogen deficiency. The  $^{13}C$  NMR data (Table 2), analyzed with the help of HSQC data, indicated 23 carbon resonances, including two ketocarbons ( $\delta_C$  199.0 and 193.3), two ester carbonyls ( $\delta_C$  170.3 and 168.8), and two olefinic carbons ( $\delta_C$  164.1 and 109.3). The remaining indices of hydrogen deficiency required another four rings. In conjunction with the HMBC data (Figure 1), a correlation between the resonances at  $\delta_H$  2.00 and  $\delta_C$  170.3, signals typical of an acetoxy group, were observed. These resonances suggested that **4** possessed a  $C_{19}$ -type quassinoid skeleton similar to that of javanicin X,<sup>16</sup> except that C-11 had an acetoxy instead of a hydroxy substituent. This was corroborated by the HMBC correlation of H-11 ( $\delta_H$  5.25) with the ester carbonyl carbon at  $\delta_C$  170.3. The NOESY cross-peaks (Figure 2) of Me-20/H-7, Me-19/H-11, Me-20/H-11, and Me-20/H-14 indicated the  $\beta$ -orientations of H-7, H-11, and H-14, and the correlations between Me-21/H-9,

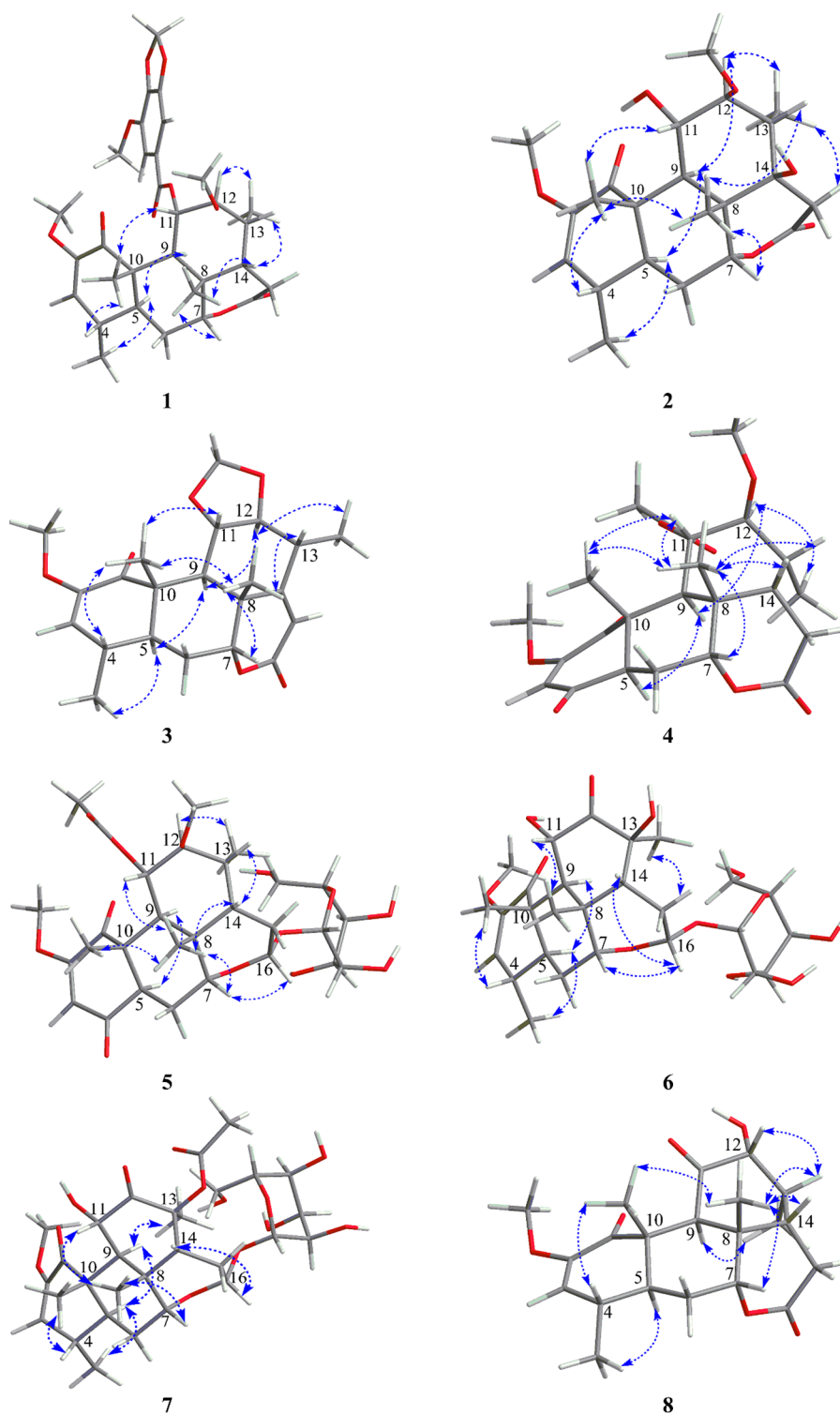


**Figure 2.** Key NOESY correlations for compounds 1–8. The 3D structures of the lowest-energy conformers were optimized at the  $\omega$ B97XD/6-311+G(d,p) level, and their relative concentrations (in percent) are according to the Boltzmann distribution (1, 48%; 2, 54%; 3, 71%; 4, 49%; 5, 46%; 6, 70%; 7, 61%; 8, 52%).

H-9/H-5, and Me-21/H-12 established the  $\alpha$ -orientation of H-5, H-9, and H-12.

The molecular formula of picrasinoside I (**5**) was confirmed to be  $C_{29}H_{42}O_{13}$  based on the  $[M + Na]^+$  ion at  $m/z$  621.2540 (calcd 621.2518) in its HRESIMS data. A glucosyl moiety was identified based on the anomeric proton resonance at  $\delta_H$  4.44 (d,  $J = 7.9$  Hz) in the  $^1H$  NMR data (Table 1) and six carbon

resonances at  $\delta_C$  97.6, 73.3, 77.0, 70.5, 76.4, and 61.1 in the  $^{13}C$  NMR data (Table 2). The  $\beta$ -anomeric configuration was deduced based on the coupling constant. An analysis of the remaining resonances of **5** suggested that its structure was similar to that of **4**, a  $C_{19}$ -type quassinoid, with the main differences occurring in the D ring. A comparison of the  $^1H$  and  $^{13}C$  NMR spectra of **5** and **4** indicated that the carbonyl at

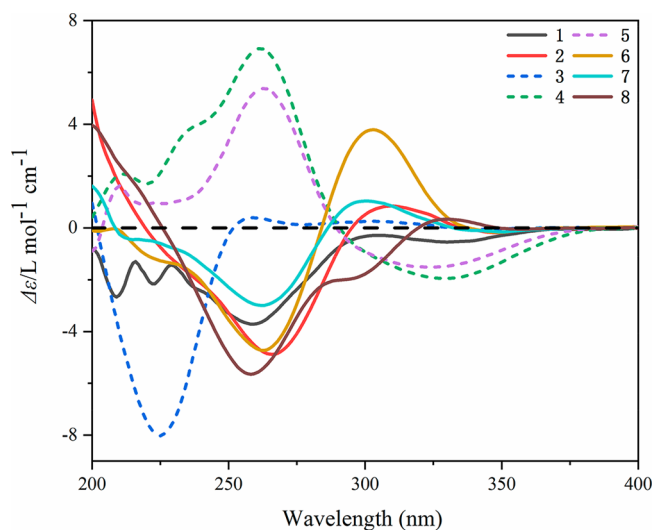


Figure 3. Experimental ECD spectra of 1–8 recorded in MeOH.

C-16 in **4** was replaced by an acetal function in **5**, which was confirmed by the HMBC correlations between H-14, H-15, and C-16 (Figure 1). The correlation of H-1'/C-16 revealed that the glucose moiety was attached at C-16. The D-configuration of the glucosyl moiety was defined by an LCNetII/ADC HPLC-OR analysis after acidic hydrolysis (Figure S73, Supporting Information). The NOESY correlations (Figure 2) indicated that **5** had the same relative configuration as **4** at C-5, C-7, C-9, C-11, C-12, and C-14. The correlation between H-14 and H-16 established H-16 as being  $\beta$ -oriented. Kumulactone D (**4**) and picrasinoside I (**5**) feature 18-nor-quassinoid scaffolds, which are the first examples of C<sub>19</sub>-type quassinoids from *P. quassioides*.

Picrasinoside J (**6**) had an ion at  $m/z$  579.2392 (calcd for C<sub>27</sub>H<sub>40</sub>O<sub>12</sub>Na, 579.2412) in its HRESIMS spectrum. By comparing its NMR data (Tables 1 and 2) with those of the known compound quassialactol,<sup>17</sup> **6** was confirmed to be the glycoside of quassialactol. In its NMR spectra, the presence of an anomeric proton at  $\delta_{\text{H}}$  4.38 (d,  $J = 7.8$  Hz) and carbon signals at  $\delta_{\text{C}}$  99.0, 73.3, 77.0, 70.0, 76.5, and 61.1 suggested that **6** is a  $\beta$ -glucoside. The glucosyl moiety was attached at C-16, as indicated by the H-16/C-1' correlation in the HMBC spectrum (Figure 1). Based on an LCNetII/ADC HPLC-OR analysis of the acidic hydrolysis products of **6**, the glucose was confirmed to be in the D-configuration (Figure S73, Supporting Information). The NOESY correlations (Figure 2) of Me-19/H-11, Me-20/H-7, Me-20/H-14, and H-14/H-16 confirmed the  $\beta$ -orientation of H-11, H-7, H-14, and H-16. The cross-peaks of H-5/H-9 and the absence of correlations between H-5 and Me-19 revealed the  $\alpha$ -orientation of H-5 and H-9.

Picrasinoside K (**7**) was determined to have a molecular formula of C<sub>29</sub>H<sub>42</sub>O<sub>13</sub> based on the  $[M + \text{Na}]^+$  ion peak at  $m/z$  621.2540 (calcd 621.2518) in its HRESIMS data. The NMR data of **7** resembled those of compound **6**. The difference was the replacement of the hydroxy moiety in **6** by an acetoxy substituent, which was supported by the downfield-shifted resonance of C-13 ( $\delta_{\text{C}}$  86.7).<sup>12</sup> In addition, its NOESY spectrum (Figure 2) revealed that **7** had the same relative configuration as **6**. The glucose was found to be in the D-configuration by an LCNetII/ADC HPLC-OR analysis of the acidic hydrolysis products of **7** (Figure S73, Supporting Information).

Interpretation of the HRESIMS and NMR data of kumulactone E (**8**) and isoparain (**10**)<sup>18</sup> revealed that they have the same

2D structures. The difference in the <sup>1</sup>H NMR and <sup>13</sup>C NMR chemical shifts suggested different configurations at C-12, which was confirmed by the NOESY correlation (Figure 2) of H-12 with H-13 and the absence of correlations between H-12 and H-9 and Me-21.

The absolute configurations of the new quassinoids **1–8** were defined by an ECD spectroscopic data analysis (Figure 3). In line with what was reported previously,<sup>1</sup> an  $\alpha,\beta$ -unsaturated lactone moiety in the D ring induces a blue-shift of the absorption bands, as is evident by comparison of the ECD spectrum of **3** with those of **1**, **2**, and **6–8**. Compounds **4** and **5** show different ECD patterns when compared to those of **1–3** and **6–8**. In a recent study, the ECD spectra of two known quassinoids were revisited to draw attention to the applicability of the ECM and some of the empirical ECD rules.<sup>13</sup> Thus, the experimental and calculated ECD data of compounds **1–8** were compared to unambiguously define the absolute configuration of the new quassinoids (Figure 4).

Kumulactone F (**9**) was first obtained as an oxidation product of nigakihemiacetal E.<sup>19</sup> It has been fully spectroscopically characterized here for the first time as a natural product (Table S1, Supporting Information).

The known compounds **10–23** were identified by a combination of spectroscopic and spectrometric methods and comparisons with reported data. The compounds were defined as isoparain (**10**),<sup>18</sup> picrasin B (**11**),<sup>10</sup> picrasinol C (**12**),<sup>10</sup> quassin (**13**),<sup>18</sup> quassilactone (**14**),<sup>20</sup> picrasinol D (**15**),<sup>10</sup> nigakilactone F (**16**),<sup>10</sup> picrasin A (**17**),<sup>21</sup> 2'-isopicrasin A (**18**),<sup>21</sup> nigakilactone L (**19**),<sup>11</sup> 14,15-dehydroquassin (**20**),<sup>22</sup> and picrasinosides B (**21**),<sup>23</sup> F (**22**),<sup>24</sup> and A (**23**).<sup>23</sup>

The neuroprotective activities of compounds **1–23** against H<sub>2</sub>O<sub>2</sub>-induced damage in SH-SY5Y cells were measured by the MTT method. Cells were preincubated with different concentrations of compounds **1–23** for 1 h, and then the cells were treated with H<sub>2</sub>O<sub>2</sub> for another 4 h. The results (Figure 5) showed that compounds **1**, **12**, **13**, **14**, and **21** had significant protective effects on SH-SY5Y cells with H<sub>2</sub>O<sub>2</sub>-induced damage at 25  $\mu\text{M}$ , and compounds **2**, **11**, **15**, **16**, **19**, **20**, **22**, and **23** had weak protective effects at particular concentrations. In terms of structure–activity relationships, compound **1**, with an aromatic substituent at C-11, had the best activity. Most of the tested quassinoids that showed neuroprotective effects possess an  $\alpha,\beta$ -unsaturated carbonyl moiety in the C ring, which suggests that this functional group may play an important part in mediating the activity. However, an  $\alpha,\beta$ -unsaturated lactone moiety in ring D was detrimental to the protective activity. For instance, the presence of an  $\alpha,\beta$ -unsaturated lactone unit in ring D of compound **3** significantly decreased its activity compared to its saturated analogue, **15**. A similar relationship was observed between compounds **20** and **13**. The structural differences among the highly oxidized quassinoids **2**, **6–10**, **15**, **16**, and **19** were mainly in the substituents on the C ring. Based on the cell viabilities after treatment with compounds **2**, **6–10**, **15**, **16**, and **19**, it can be concluded that the presence of a ketocarbonyl group in the C ring was not conducive for the protective activity since compounds **6–10** were less active than compounds **2**, **15**, **16**, and **19**.

As shown in Figure 5, compounds **1**, **12–14**, and **21** had more potential against H<sub>2</sub>O<sub>2</sub>-induced neuronal cell damage than their analogues at a concentration of 25  $\mu\text{M}$ . Further flow cytometry analysis was performed to explore the effect of quassinoids on H<sub>2</sub>O<sub>2</sub>-induced apoptosis. The results indicated that these compounds markedly decrease the apoptotic ratio in

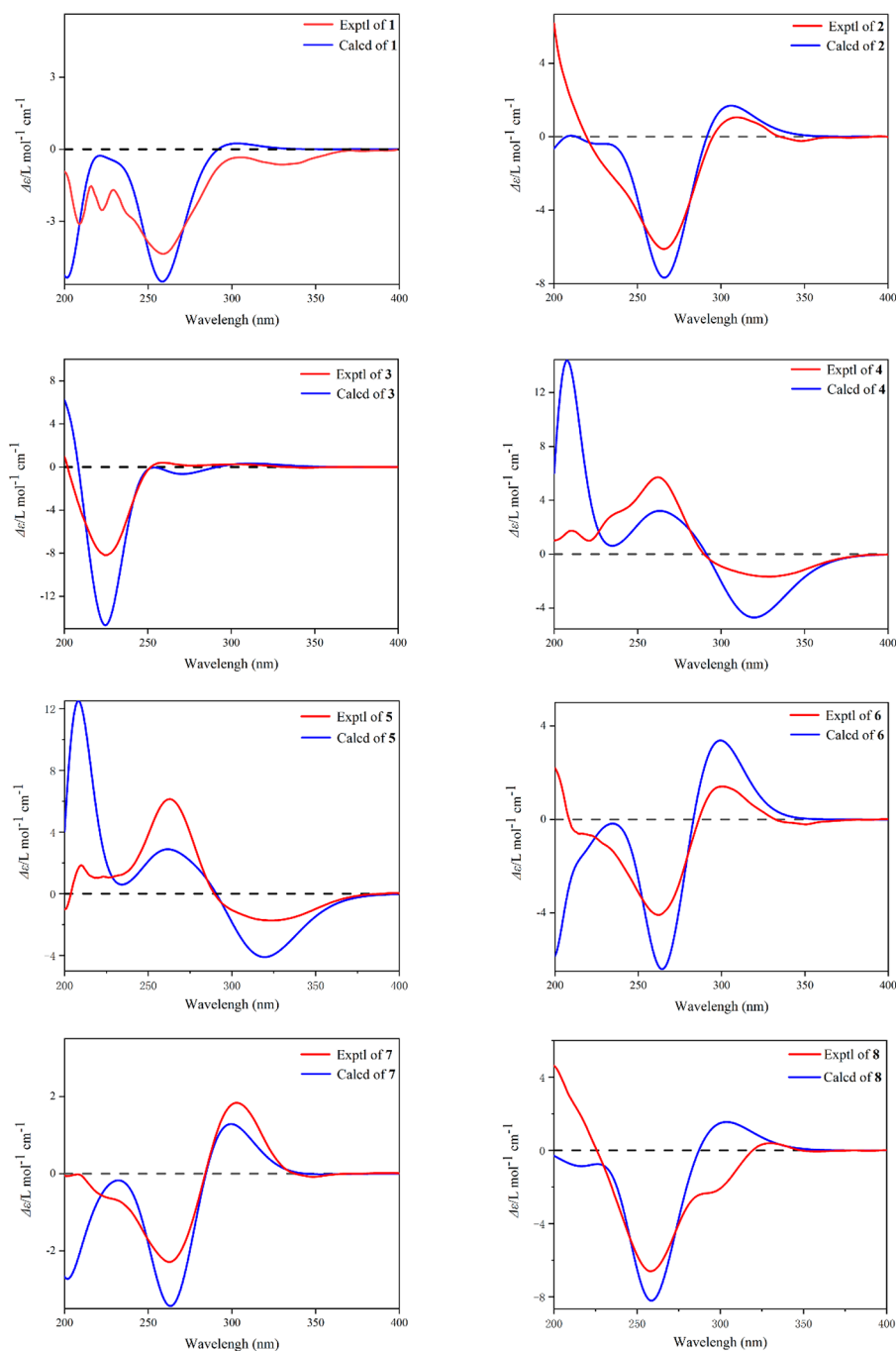


**Figure 4.** Comparison of the experimental and calculated ECD spectra of compounds **1**–**8** in MeOH. Spectra were calculated at the CAM-B3LYP/def2-TZVP// $\omega$ B97X-D/6-311+G(d,p) level.

H<sub>2</sub>O<sub>2</sub>-treated SH-SY5Y cells (Figure 6). The quassinoid glucoside **21** was more active than the corresponding aglycone **13**. Compound **1** reduced the H<sub>2</sub>O<sub>2</sub>-induced apoptosis rate from 27.2% to 10.3%, demonstrating that an aromatic substituent at C-11 has a significant effect on the activity. The results showed that these compounds could reduce the amount of apoptotic cells induced by H<sub>2</sub>O<sub>2</sub> treatment.

H<sub>2</sub>O<sub>2</sub> was proven to activate caspase-3 to induce SH-SY5Y cell apoptosis.<sup>25</sup> Consequently, a caspase-3 activity assay kit was used to quantitatively measure the activity of caspase-3 in the apoptotic cells. As shown in Figure 7, in H<sub>2</sub>O<sub>2</sub>-treated cells, the caspase-3 activity notably increased, while a significant decrease was observed following treatment with **1** and **21**. All

these results suggest that compounds **1** and **21** can counteract H<sub>2</sub>O<sub>2</sub>-induced apoptosis through regulating caspase-3. This is the first report on quassinoids with neuroprotective activities. The findings extend the medicinal value of quassinoids and *P. quassioides*.

## EXPERIMENTAL SECTION

**General Experimental Procedures.** The general experimental procedures are listed in the Supporting Information.

**Plant Material.** The dried stems of *P. quassioides* were collected from Anhui Province, China, in November 2015. Plant identification was done by Professor Jincai Lu at Shenyang Pharmaceutical University. A voucher specimen (no. 20151101) has been deposited

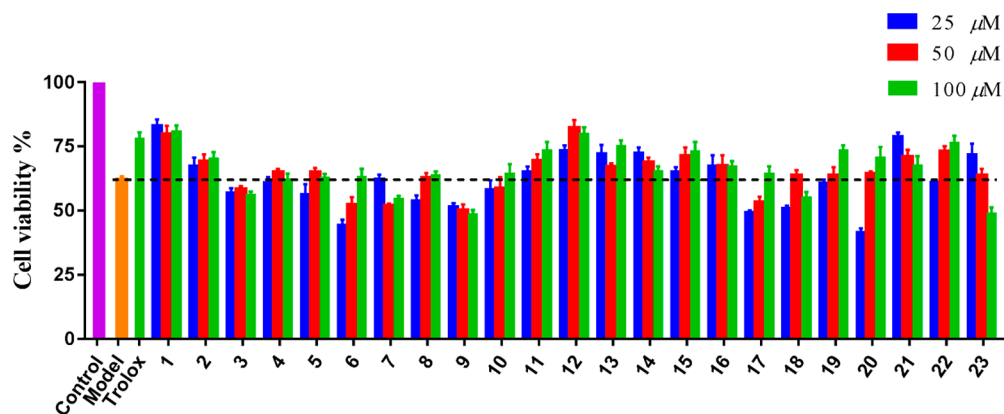


**Figure 5.** Neuroprotective effects of compounds 1–23 against  $\text{H}_2\text{O}_2$ -induced injury in SH-SY5Y cells. After  $\text{H}_2\text{O}_2$  ( $300 \mu\text{M}$ ) treatment, the cell viabilities were determined by an MTT assay in the presence or absence of the test compounds at different concentrations (25, 50, and  $100 \mu\text{M}$ ). Trolox was used as the positive control.

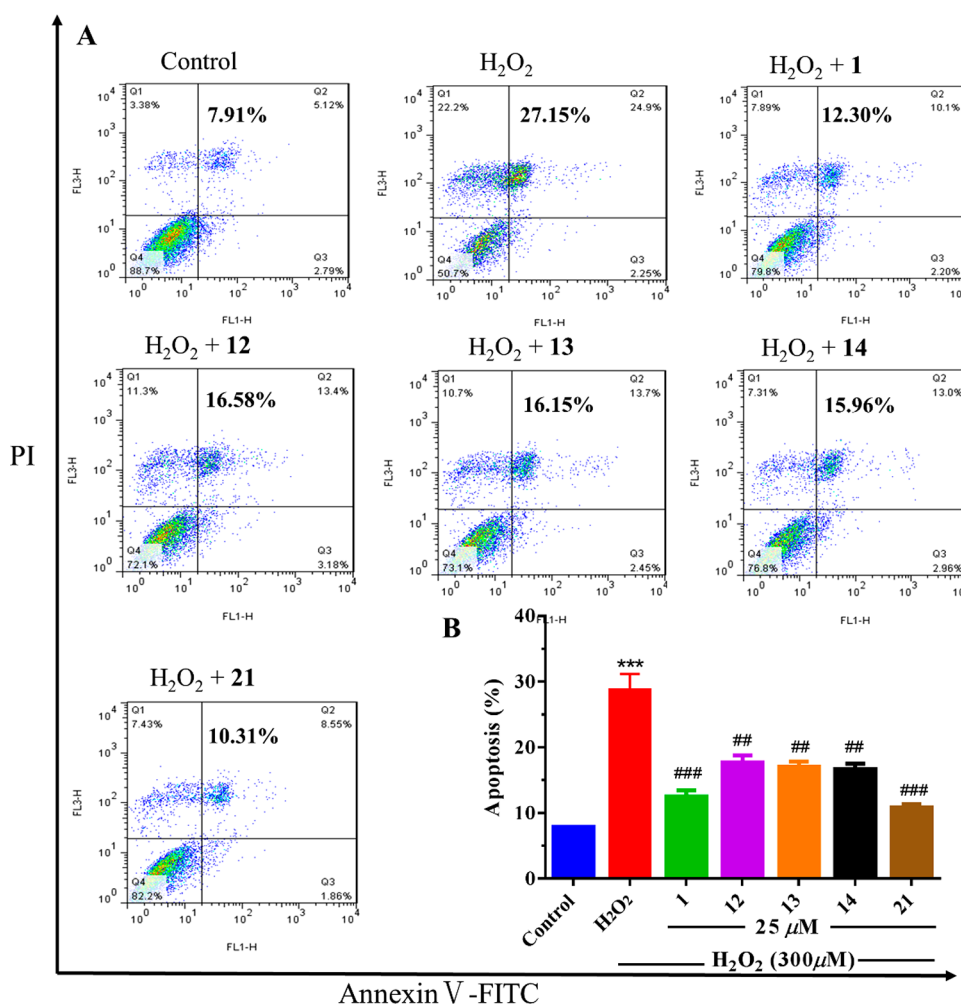


**Figure 6.** Annexin V-FITC/PI double staining analysis was applied to detect apoptotic cells in SH-SY5Y cells treated with 1, 12–14, and 21 ( $25 \mu\text{M}$ ) prior to treatment with  $300 \mu\text{M}$   $\text{H}_2\text{O}_2$  for 4 h. (A) Representative pictures were obtained from flow cytometry. (B) Quantitative analysis of the apoptotic ratio. The apoptosis ratio is reported as the mean  $\pm$  SD. \*\*\* $P < 0.001$  compared with control; ## $P < 0.01$ , ### $P < 0.001$  compared with  $\text{H}_2\text{O}_2$ -treated cells.

in the School of Traditional Chinese Materia Medica, Shenyang Pharmaceutical University.

**Extraction and Isolation.** The dried stems of *P. quassioides* (30.0 kg) were extracted with 95% EtOH ( $3 \times 50 \text{ L} \times 4 \text{ h}$ ) at  $50^\circ\text{C}$ . The detailed process of isolation is described in the Supporting Information.

(4*S*,5*S*,7*R*,8*S*,9*S*,10*S*,11*S*,12*S*,13*R*,14*S*)-Kumulactone A (1): white powder,  $[\alpha]_{\text{D}}^{20} -38$  ( $c$  0.2, MeOH); UV (MeOH)  $\lambda_{\text{max}}$  ( $\log \epsilon$ ) 271 (0.911) nm; ECD (MeOH,  $\Delta\epsilon$ )  $\lambda_{\text{max}}$  256 ( $-4.26$ ) nm; IR (KBr)  $\nu_{\text{max}}$  3440, 2962, 2937, 1733, 1706, 1632, 1609, 1431, 1325, 1259, 1180, 1042  $\text{cm}^{-1}$ ;  $^1\text{H}$  and  $^{13}\text{C}$  NMR, see Tables 1 and 2; HRESIMS  $m/z$  593.2338  $[\text{M} + \text{Na}]^+$  (calcd for  $\text{C}_{31}\text{H}_{38}\text{NaO}_{10}$ , 593.2357).

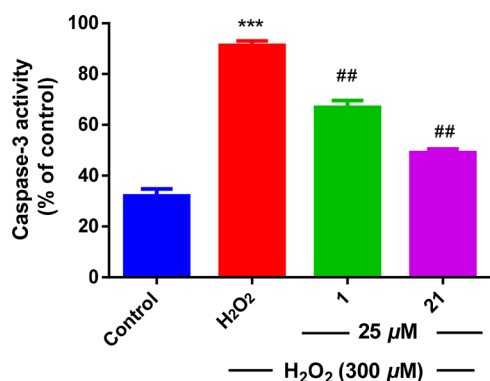


**Figure 7.** Caspase-3 activity of SH-SY5Y cells treated with H<sub>2</sub>O<sub>2</sub> and/or compounds **1** and **21**. Data are presented as the means  $\pm$  SDs. \*\*\**P* < 0.001 compared with control; ##*P* < 0.01 compared with H<sub>2</sub>O<sub>2</sub>-treated cells.

(4*S*,5*S*,7*R*,8*R*,9*S*,10*S*,11*S*,12*S*,13*S*,14*R*)-Kumulactone **B** (**2**): white powder,  $[\alpha]_D^{20} +32$  (*c* 0.4, MeOH); UV (MeOH)  $\lambda_{\max}$  (log  $\epsilon$ ) 271 (0.911) nm; ECD (MeOH,  $\Delta\epsilon$ )  $\lambda_{\max}$  259 (−3.89), 308 (+0.67) nm; IR (KBr)  $\nu_{\max}$  3444, 2984, 1708, 1606, 1492, 1396, 1371, 1273, 1238, 1174, 1115 cm<sup>−1</sup>; <sup>1</sup>H and <sup>13</sup>C NMR, see Tables 1 and 2; HRESIMS *m/z* 431.2054 [M + Na]<sup>+</sup> (calcd for C<sub>22</sub>H<sub>32</sub>NaO<sub>7</sub>, 431.2040).

(4*S*,5*S*,7*R*,8*R*,9*S*,10*S*,11*S*,12*S*,13*R*)-Kumulactone **C** (**3**): white powder,  $[\alpha]_D^{20} -8$  (*c* 0.8, MeOH); UV (MeOH)  $\lambda_{\max}$  (log  $\epsilon$ ) 261 (1.12) nm; ECD (MeOH,  $\Delta\epsilon$ )  $\lambda_{\max}$  227 (−6.92) nm; IR (KBr)  $\nu_{\max}$  3425, 2964, 2938, 2881, 1721, 1706, 1632, 1450, 1371, 1355, 1260, 1239, 1114, 1036 cm<sup>−1</sup>; <sup>1</sup>H and <sup>13</sup>C NMR, see Tables 1 and 2; HRESIMS *m/z* 411.1789 [M + Na]<sup>+</sup> (calcd for C<sub>22</sub>H<sub>28</sub>NaO<sub>6</sub>, 411.1778).

(5*R*,7*R*,8*S*,9*S*,10*R*,11*S*,12*S*,13*R*,14*S*)-Kumulactone **D** (**4**): white powder,  $[\alpha]_D^{20} +33$  (*c* 0.2, MeOH); UV (MeOH)  $\lambda_{\max}$  (log  $\epsilon$ ) 262 (1.12) nm; ECD (MeOH,  $\Delta\epsilon$ )  $\lambda_{\max}$  257 (+6.67) nm; IR (KBr)  $\nu_{\max}$  3431, 2986, 1608, 1492, 1441, 1400, 1367, 1173, 1006, 799 cm<sup>−1</sup>; <sup>1</sup>H and <sup>13</sup>C NMR, see Tables 1 and 2; HRESIMS *m/z* 457.1808 [M + Na]<sup>+</sup> (calcd for C<sub>23</sub>H<sub>30</sub>NaO<sub>8</sub>, 457.1833).

(5*R*,7*R*,8*S*,9*S*,10*R*,11*S*,12*S*,13*R*,14*S*,16*S*)-Picrasinoside **I** (**5**): yellow powder,  $[\alpha]_D^{20} -1$  (*c* 0.1, MeOH); UV (MeOH)  $\lambda_{\max}$  (log  $\epsilon$ ) 260 (1.30) nm; ECD (MeOH,  $\Delta\epsilon$ )  $\lambda_{\max}$  261 (+5.33) 323 (−1.60) nm; IR (KBr)  $\nu_{\max}$  3427, 2986, 1611, 1492, 1441, 1400, 1366, 1173, 1006, 799 cm<sup>−1</sup>; <sup>1</sup>H and <sup>13</sup>C NMR, see Tables 1 and 2; HRESIMS *m/z* 621.2540 [M + Na]<sup>+</sup> (calcd for C<sub>29</sub>H<sub>42</sub>NaO<sub>13</sub>, 621.2518).

(4*S*,5*S*,7*R*,8*R*,9*S*,10*S*,11*S*,13*S*,14*R*,16*S*)-Picrasinoside **K** (**6**): white powder,  $[\alpha]_D^{20} -6$  (*c* 0.4, MeOH); UV (MeOH)  $\lambda_{\max}$  (log  $\epsilon$ ) 269 (1.13) nm; ECD (MeOH,  $\Delta\epsilon$ )  $\lambda_{\max}$  256 (−8.02) 300 (+2.83) nm; IR (KBr)  $\nu_{\max}$  3416, 2984, 2929, 1728, 1673, 1632, 1614, 1492, 1442, 1396, 1368, 1237, 1172, 1122, 1040, 1024 cm<sup>−1</sup>; <sup>1</sup>H and <sup>13</sup>C NMR, see Tables 1 and 2; HRESIMS *m/z* 579.2392 [M + Na]<sup>+</sup> (calcd for C<sub>27</sub>H<sub>40</sub>NaO<sub>12</sub>, 579.2412).

(4*S*,5*S*,7*R*,8*R*,9*S*,10*S*,11*S*,13*S*,14*R*,16*S*)-Picrasinoside **J** (**7**): light yellow powder,  $[\alpha]_D^{20} -3$  (*c* 0.3, MeOH); UV (MeOH)  $\lambda_{\max}$  (log  $\epsilon$ ) 275 (1.02) nm; ECD (MeOH,  $\Delta\epsilon$ )  $\lambda_{\max}$  256 (−2.89) 303 (+2.00) nm; IR (KBr)  $\nu_{\max}$  3428, 2986, 1611, 1492, 1441, 1400, 1367, 1173, 1007, 799 cm<sup>−1</sup>; <sup>1</sup>H and <sup>13</sup>C NMR, see Tables 1 and 2; HRESIMS *m/z* 621.2506 [M + Na]<sup>+</sup> (calcd for C<sub>29</sub>H<sub>42</sub>NaO<sub>13</sub>, 621.2518).

(4*S*,5*S*,7*R*,8*S*,9*S*,10*S*,12*R*,13*R*,14*S*)-Kumulactone **E** (**8**): yellow powder,  $[\alpha]_D^{20} -46$  (*c* 0.3, MeOH); UV (MeOH)  $\lambda_{\max}$  (log  $\epsilon$ ) 263 (1.27) nm; ECD (MeOH,  $\Delta\epsilon$ )  $\lambda_{\max}$  256 (−5.32) nm; IR (KBr)  $\nu_{\max}$  3424, 2986, 1611, 1492, 1441, 1399, 1367, 1173, 1006, 799 cm<sup>−1</sup>; <sup>1</sup>H and <sup>13</sup>C NMR, see Tables 1 and 2; HRESIMS *m/z* 399.1763 [M + Na]<sup>+</sup> (calcd for C<sub>21</sub>H<sub>28</sub>NaO<sub>6</sub>, 399.1778).

**Neuroprotective Activity Assay.** The protective activities of the 23 quassinoids toward SH-SY5Y cells damaged by H<sub>2</sub>O<sub>2</sub> were examined following the reported procedures.<sup>26</sup>

**Apoptosis Analysis.** The apoptosis analysis was carried out by an annexin V-FITC/PI double staining assay as described previously.<sup>27</sup>

**Caspase-3 Activity Assay.** For compounds **1** and **21**, the caspase-3 activity was carried out following the methods described by Xu et al.<sup>28</sup>

## ASSOCIATED CONTENT

### Supporting Information

The Supporting Information is available free of charge on the ACS Publications website at DOI: 10.1021/acs.jnatprod.8b00470.

Additional figures and a table (PDF)

## AUTHOR INFORMATION

### Corresponding Authors

\*E-mail: xiaoxiao270@163.com (X.-X. Huang).

\*E-mail: songsj99@163.com (S.-J. Song).

### ORCID

Shao-Jiang Song: 0000-0002-9074-2467

### Notes

The authors declare no competing financial interest.

## ACKNOWLEDGMENTS

This project was funded by the National Nature Science Foundation (81872767) of China and the Career Development Support Plan for Young and Middle-aged Teachers in Shenyang Pharmaceutical University (ZQN2018006).

## REFERENCES

- Xu, J.; Xiao, D.; Song, W.; Chen, L.; Liu, W.; Xie, N.; Feng, F.; Qu, W. *Fitoterapia* **2016**, *110*, 13–19.
- Xu, J.; Xiao, D.; Lin, Q.; He, J.; Liu, W.; Xie, N.; Feng, F.; Qu, W. *J. Nat. Prod.* **2016**, *79*, 1899–1910.
- Jiao, W.; Chen, G.-D.; Gao, H.; Li, J.; Gu, B.; Xu, T.; Yu, H.; Shi, G.; Yang, F.; Yao, X.; Lin, H. *J. Nat. Prod.* **2014**, *77*, 2707–2712.
- Yoshikawa, K.; Sugawara, S.; Arihara, S. *Phytochemistry* **1995**, *40*, 253–256.
- Polonsky, J. *Fortschr. Chem. Org. Naturst.* **1985**, *47*, 221–264.
- Polonsky, J. *Fortschr. Chem. Org. Naturst.* **1973**, *30*, 101–150.
- Guo, Z.; Vangapandu, S.; Sindelar, R. W.; Walker, L. A.; Sindelar, R. D. *Curr. Med. Chem.* **2005**, *12*, 173–190.
- Koreeda, M.; Harada, N.; Nakanishi, K. *J. Am. Chem. Soc.* **1974**, *96*, 266–268.
- Hikino, H.; Ohta, T.; Takemoto, T. *Phytochemistry* **1975**, *14*, 2473–2481.
- Daido, M.; Fukamiya, N.; Okano, M.; Tagahara, K. *J. Nat. Prod.* **1992**, *55*, 1643–1647.
- Daido, M.; Fukamiya, N.; Okano, M.; Tagahara, K. *J. Nat. Prod.* **1995**, *58*, 605–608.
- Yang, S.; Yue, J. *Helv. Chim. Acta* **2004**, *87*, 1591–1600.
- Pescitelli, G.; Di Bari, L. *Chirality* **2017**, *29*, 476–485.
- Pescitelli, G.; Di Bari, L. *J. Nat. Prod.* **2017**, *80*, 2855–2859.
- Muraa, T.; Tsuyuki, T.; Nishihama, T.; Masuda, S.; Takahashi, T. *Tetrahedron Lett.* **1969**, *10*, 3013–3016.
- Koike, K.; Ishii, k.; mitsunaga, k.; Ohmoto, T. *Chem. Pharm. Bull.* **1991**, *39*, 2021–2023.
- Dou, J.; McChesney, J.; Sindelar, R.; Goins, D. K.; Khan, L.; Walker, L. *Int. J. Pharmacogn.* **1996**, *34*, 349–354.
- Barbetti, P.; Grandolini, G.; Fardella, G.; Chiappini, I. *Phytochemistry* **1993**, *32*, 1007–1013.
- Muraa, T.; Sugie, A.; Tsuyuki, T.; Takahashi, T. *Chem. Pharm. Bull.* **1975**, *23*, 2188–2190.
- Lang'at-Thoruwa, C.; Kirby, G. C.; Phillipson, J. D.; Warhurst, D. C.; Watt, R. A.; Wright, C. W. *J. Nat. Prod.* **2003**, *66*, 1486–1489.
- Jiao, W.; Gao, H.; Zhao, F.; He, F.; Zhou, G.; Yao, X. *Chem. Biodiversity* **2011**, *8*, 1163–1169.
- Robins, R. J.; Rhodes, M. J. *J. Chromatogr. A* **1984**, *283*, 436–440.

- (23) Matsuzaki, T.; Fukamiya, N.; Okano, M.; Fujita, T.; Tagahara, K.; Lee, K. H. *J. Nat. Prod.* **1991**, *54*, 844–888.
- (24) Okano, M.; Fujita, T.; Fukamiya, N.; Aratani, T. *Bull. Chem. Soc. Jpn.* **1985**, *58*, 1793–1800.
- (25) Dalle-Donne, I.; Rossi, R.; Colombo, R.; Giustarini, D.; Milzani, A. *Clin. Chem.* **2006**, *52*, 601–623.
- (26) Huang, X. X.; Ren, Q.; Song, X. Y.; Zhou, L.; Yao, G. D.; Wang, X. B.; Song, S. J. *Fitoterapia* **2018**, *125*, 6–12.
- (27) Qi, X. L.; Zhang, Y. Y.; Zhao, P.; Zhou, L.; Wang, X. B.; Huang, X. X.; Lin, B.; Song, S. J. *J. Nat. Prod.* **2018**, *81*, 1225–1234.
- (28) Xu, X. H.; Zhang, L. L.; Wu, G. S.; Chen, X.; Li, T.; Chen, X.; Wang, Y. T.; Lu, J. *Planta Med.* **2017**, *83*, 254–260.